

## Differential rotation in giant planets maintained by density-stratified turbulent convection

GARY A. GLATZMAIER\*<sup>†</sup>, MARTHA EVONUK<sup>‡</sup> and TAMARA M. ROGERS<sup>§</sup>

<sup>†</sup>Earth and Planetary Sciences Department, University of California,  
1156 High Street, Santa Cruz, CA 95064, USA

<sup>‡</sup>Institut für Geophysik, ETH Zürich Hönggerberg,  
8093 Zürich, Switzerland

<sup>§</sup>High Altitude Observatory, National Center for Atmospheric Research,  
3080 Center Green Drive, Boulder, CO 80301, USA

(Received 18 September 2007; in final form 12 March 2008)

The zonal winds on the surfaces of giant planets vary with latitude. Jupiter and Saturn, for example, have several bands of alternating eastward (prograde) and westward (retrograde) jets relative to the angular velocity of their global magnetic fields. These surface wind profiles are likely manifestations of the variations in depth and latitude of angular velocity deep within the liquid interiors of these planets. Two decades ago it was proposed that this differential rotation could be maintained by vortex stretching of convective fluid columns that span the interiors of these planets from the northern hemisphere surface to the southern hemisphere surface. This now classic mechanism explains the differential rotation seen in laboratory experiments and in computer simulations of, at best, weakly turbulent convection in rotating constant-density fluid spheres. However, these experiments and simulations are poor approximations for the density-stratified strongly-turbulent interiors of giant planets. The long thin global convective columns predicted by the classic geostrophic theory for these planets would likely not develop. Here we propose a much more robust mechanism for maintaining differential rotation in radius based on the local generation of vorticity as rising plumes expand and sinking plumes contract. Our high-resolution two-dimensional computer simulations demonstrate how this mechanism could maintain either prograde or retrograde surface winds in the equatorial region of a giant planet depending on how the density scale height varies with depth.

**Keywords:** Giant planet interiors, differential rotation, density-stratification

### 1 Introduction

The complicated flow patterns observed at the cloud tops of giant planets are likely due to a combination of atmospheric phenomena in the shallow surface layer and thermal convection within the deep interior. The question, which has been debated for several decades, is what differential rotation exists deep below the surface of a giant planet and what dynamics maintains it. Differential rotation is the axisymmetric zonal wind pattern in latitude and radius relative to the deep-seated global magnetic field, which is assumed to be rotating at approximately the mean rotation rate of the planet. Differential rotation can be maintained by either axisymmetric Coriolis forces arising from a thermally-driven meridional circulation, i.e., as a thermal wind, or by the convergence of Reynolds stress, i.e., the nonlinear transport of longitudinal momentum in latitude and radius. Magnetic forces, like viscous forces, typically inhibit differential rotation; however in some cases they too can drive differential rotation (e.g. Dormy *et al.* 2002).

Most theoretical studies of this problem have approached it from an Earth-atmosphere context, ignoring the dynamics of the vast interior and using models and approximations only appropriate for shallow atmospheres. See Dowling (1995) for a review of this approach. These models typically assume a hydrostatic balance in the radial direction instead of solving the full momentum equation. That is, they ignore the radial component of the flow in transporting longitudinal momentum or producing Coriolis forces, two critical elements for maintaining differential rotation in deep convective zones. Instead, these shallow-atmosphere models of giant planets usually rely on a thermal wind scenario (e.g. Allison 2000) or the convergence of latitude-longitude Reynolds stress to drive zonal winds. The latter produces a retrograde

---

\*Corresponding author. Email: glatz@es.ucsc.edu

(i.e., westward directed) zonal wind in the equatorial region (e.g. Williams 1978, Cho and Polvani 1996) because the local vertical component of the planetary rotation rate (the only component these models consider) increases with latitude. Retrograde zonal flow in the equatorial region is observed on surfaces of Uranus and Neptune (Hammel *et al.* 2005) but a prograde (i.e., eastward directed) equatorial jet is observed on our gas giants, Jupiter (Porco *et al.* 2003) and Saturn (Sanchez-Lavega *et al.* 2000). The zonal wind at higher latitudes on the gas giants has a latitudinally banded pattern of alternating retrograde and prograde flows. A banded pattern of zonal flows with a prograde equatorial jet can be obtained by tuning a heating function distributed in latitude and radius that continually nudges the temperature toward a prescribed profile that drives the desired zonal wind pattern (e.g. Williams 2003). However, in such a model the zonal wind profile in latitude and radius is the result of the shallow layer assumption and the mathematical fit to the surface observations via the ad hoc heating function; therefore it does not provide a dynamically-consistent prediction or explanation.

It may indeed be the case that the zonal winds on giant planets are confined to the shallow surface layers and driven by heat sources and instabilities there without any influence from the deep convection below. However, hydrostatic shallow-atmosphere models assume this from the start and so are not capable of predicting this to be the case. The Galileo probe measured a doubling of the zonal wind speed with depth in the surface layer of Jupiter (Atkinson *et al.* 1998). A scale analysis (Ingersoll and Pollard 1982) suggests that the zonal winds on Jupiter and Saturn extend well below their surfaces. Probably the strongest indication of the existence of deep convection is that spherically symmetric evolutionary models with detailed equations of state and opacities predict convection throughout the deep fluid interiors of our gas giants (e.g. Hubbard *et al.* 1999, Guillot 2005, and T. Guillot private communication). Therefore, to predict what differential rotation exists below the surface and to understand how it is maintained one needs a global dynamically-consistent model that extends deep below the surface, with sufficient physics and the full set of three-dimensional (3D) equations of motion. The model may also need good representations of radiative transfer and moist convection near the surface (Ingersoll *et al.* 2000), a hydrogen phase transition well below the surface separating the semi-conducting and metallic regions (Nellis 2000) and magnetic field generation with its feedback on the flow.

An alternative to a shallow-atmosphere model is a dynamically-consistent 3D global model from the geodynamo community. Most giant planet studies using this approach apply the Boussinesq approximation to the set of equations that describes deep rotating convection. That is, a constant background density is assumed. These 3D global models do produce banded zonal winds and a prograde equatorial jet without neglecting the dynamics of the deep interior and without prescribing ad hoc heating distribution functions (e.g. Sun *et al.* 1993, Christensen 2002, Stanley and Bloxham 2004, Heimpel *et al.* 2005). The studies find that the convergence of Reynolds stress, both latitude-longitude and radius-longitude, dominates over the thermal wind mechanism in maintaining differential rotation and that the kinetic energy in the meridional circulation is typically several orders of magnitude less than that in the differential rotation (e.g. Christensen 2002). That is, these studies suggest that meridional circulation is maintained by the Coriolis forces arising from the differential rotation, not the other way around (i.e., the differential rotation is not a thermal wind). However, because these Boussinesq models assume a constant background density and relatively large viscosity, the differential rotation in these simulations is maintained by the vortex stretching of large convective columns due to the sloping impermeable boundary.

Unlike these Boussinesq models, the interior of a giant planet has a significant density stratification, especially near the surface, and much smaller viscosity, which produces strong convective turbulence characterized by a broad spectrum of scales (e.g. Glatzmaier 2005). This turbulence is dominated by small-scale fluid parcels, which initially develop as thermal boundary layer instabilities, then detach and either rise from the inner boundary or sink from the outer boundary. Their dynamical evolution in the bulk of the convection zone is determined by nonlinear vortex-vortex interactions and the local density stratification, not by the spherical curvature of distant boundaries. The deep-convection constant-density models from the geodynamo community produce flow amplitudes relatively independent of depth, opposite of that assumed in the hydrostatic shallow-atmosphere models from the climate community. Both, however, completely ignore the maintenance of differential rotation by radial flow through a density stratification.

Glatzmaier and Gilman (1981, 1982), using quasi-linear solutions to the anelastic equations of motion,

examined the role of density stratification in generating vorticity and maintaining differential rotation by compressional torque without requiring the vortex stretching of columnar convection. Ingersoll and Pollard (1982) and Busse (1986) addressed the role of density stratification using scale and asymptotic analyses. However, they retained Busse's original assumption of vortex-stretching by geostrophic columnar convection spanning the entire interior, replacing the column length by the integrated column mass.

Here we examine the deficiency of the classic vortex-stretching mechanism for maintaining differential rotation in giant planets. Then we describe a more robust mechanism that accounts for their large density stratifications and strong turbulence without requiring geostrophic columns that span the interior. We study this mechanism with nonlinear simulations of turbulent convection that focus on the convergence of radial-longitudinal Reynolds stress for maintaining differential rotation in radius.

## 2 The classic vortex-stretching mechanism

3D constant-density Boussinesq models rely on the classic vortex-stretching mechanism (Busse 1983, 2002) to generate vorticity and maintain differential rotation. That mechanism requires thermal convection in the form of vortex columns, with axes parallel to the planet's axis of rotation, spanning from the northern to southern boundary surfaces. Vorticity is generated by the deformation the fluid experiences parallel to the rotation axis as it circulates within these global columns. The curvature of the impermeable spherical boundaries is responsible for the longitudinal tilt of the columnar flow and the resulting convergence of prograde angular momentum in the outer regions and retrograde angular momentum in the inner regions. This type of columnar convection naturally develops when the Coriolis and pressure gradient forces nearly balance everywhere and all other forces are relatively small, i.e., when the flow is geostrophic. The classic Proudman-Taylor theorem (Proudman 1916) for incompressible fluid then predicts, to first order, that fluid flow is within planes parallel to the equatorial plane.

However, it is unlikely that the classic vortex-stretching mechanism plays a role in the low-viscosity turbulently-convecting interiors of giant planets (or stars) because these columns would be extremely thin. If they would develop, they would quickly become unstable, buckle and shred apart into many short unconnected vortices because nonlinear inertial effects are not negligible at scales as small as the column diameters. That is, although the amplitudes of the deep convective velocities may be small, their gradients are not.

To estimate the typical diameter of convective columns in a giant planet, we choose Jupiter-like values for the molecular viscosity (Stevenson 1982),  $\nu = 10^{-6} \text{m}^2 \text{s}^{-1}$ , planetary rotation rate,  $\Omega = 10^{-4} \text{s}^{-1}$ , and radius,  $R = 10^8 \text{m}$ . This makes the Ekman number,  $\text{Ek} = \nu / (2\Omega R^2)$ , about  $10^{-18}$ . If one then adopts the theoretical prediction (Roberts 1968, Busse 1970) that the diameter of convective columns (at onset of convection) should go like  $\text{Ek}^{1/3} R$ , these columns would have diameters of roughly 100m, a million times smaller than their lengths. Of course convection in giant planets is not at its onset, so one might invoke a turbulent (eddy) viscosity many orders of magnitude greater than the molecular value to obtain a column diameter comparable to the latitudinal scale of the observed zonal jets. However, even if one assumed the largest possible turbulent viscosity equal to the product of the column diameter,  $D$ , and its convective velocity normal to the axis,  $v_r$ , which is estimated to be of order  $10^{-3} \text{ms}^{-1}$  deep below the surface based on the observed heat flux (Starchenko and Jones 2002), the convective column diameters,

$$D \approx \left( \frac{v_r R}{\Omega} \right)^{1/2},$$

would be several thousand times smaller than their lengths.

Alternatively, if one acknowledges the strongly nonlinear nature of convection in our rapidly rotating giant planets, one would balance the generation of local non-axisymmetric vorticity by Coriolis forces with the advection of this vorticity. In these constant-density models, for which  $\nabla \cdot \mathbf{v}$  vanishes, vorticity is assumed to be generated by the classic vortex-stretching mechanism. The stretching torque goes like

$$\Omega \frac{\partial v_z}{\partial z} \approx \frac{\Omega v_r}{L_{stretch}}$$

where  $z$  and  $r$  are the cylindrical coordinates parallel and perpendicular to  $\mathbf{\Omega}$ , respectively, and  $v_z$  is the secondary fluid flow parallel to the column (i.e., the stretching velocity).  $L_{stretch}$  is the geometric length scale in the  $r$  direction for column stretching due to the spherical boundaries; it is equal to  $|d \ln H / dr|^{-1} = (R^2 - r^2)/r$ , where  $H$  is the column length,  $2(R^2 - r^2)^{1/2}$  (Busse, 2002).  $L_{stretch}$  varies considerably with latitude; it is approximately the planetary radius for columns intersecting the surface at mid-latitude. This vorticity generation would be balanced with the advection by velocity  $\mathbf{V}$  of vorticity  $\nabla \times \mathbf{v}$ , which has an approximate amplitude of  $V v_r / D^2$ . The balance gives the Rhines-like scale (Rhines 1975, Heimpel *et al.* 2005) for the column diameters of

$$D \approx \left( \frac{V L_{stretch}}{\Omega} \right)^{1/2} \quad \text{and} \quad \frac{D}{H} \approx \left( \frac{V}{4\Omega r} \right)^{1/2} .$$

This assumes the banded zonal wind, i.e. the differential rotation which acts to destroy the columnar flow structures by shearing them, is balanced by their generation via vortex stretching. If one chooses  $V$  to be the maximum zonal wind speed on Jupiter's surface,  $100\text{ms}^{-1}$ , the diameter of columns intersecting the surface at low latitude would be about a hundred times smaller than  $R$  and about twenty times smaller than their lengths.

These vortex-stretching arguments have been based on the constant-density approximation for a giant planet's interior and an impermeable outer boundary. However, unlike laboratory experiments and previous 3D computer models, the surfaces of giant planets are not strictly impermeable. It is unlikely that flows in the low-density highly-compressible strongly-turbulent surface region of a giant planet could drive the  $z$ -directed secondary flow in the much denser fluid deep below the surface required for the vortex-stretching mechanism.

If one does acknowledge the large density stratifications in our giant planets, local vorticity is easily generated by compressional torque:

$$-2\mathbf{\Omega} \nabla \cdot \mathbf{v} .$$

This is proportional to the radial component of convective velocity ( $v_r$ ) and inversely proportional to the local density scale height,  $L_{compress}$  (see Appendix A). If, at low latitude, the amplitude of vorticity were again approximated as convective velocity ( $v_r$ ) divided by the vortex diameter, balancing this compressional torque with the advection of vorticity would make the typical vortex diameter be

$$D \approx \left( \frac{V L_{compress}}{\Omega} \right)^{1/2} .$$

Since the local density scale height is very small in the outer region of Jupiter (Bodenheimer *et al.* 2003, Guillot 2005, T. Guillot private communication) the characteristic diameter of vortices in the shallow equatorial region would be a thousand times smaller than Jupiter's radius  $R$ . However, unlike the geostrophic vortex-stretching mechanism, this compressional-torque mechanism does not require vortices spanning from the northern to the southern boundaries. Small vortices aligned with the planet's rotation axis likely *do* exist within its turbulent interior; but most are likely short isolated structures.

One might imagine geostrophic columns close to the planetary rotation axis. Fluid circulating in such columns at low latitude (i.e., in the deep interior) would span only a fraction of a density scale height. At high latitude, where the density scale height is small, the flow would be mainly in latitude; therefore again fluid parcels would experience little density stratification. However, the relative change in volume experienced by fluid parcels circulating in cylindrical radius within such columns would vary along the

length of the column, depending on the parcel's latitude and on the planet's density profile in spherical radius. This will generate vorticity via compressional torque at rates that vary along the column length and therefore would likely cause the columns to buckle and shear apart.

In this simple scale analysis we have been assuming the cross sections of vortices are roughly circular. However, a significant differential rotation would likely shear them into vortex sheets. In such a scenario their longitudinal dimensions and velocities would be much larger than those in cylindrical radius.

### 3 The density-stratification mechanism

The alternative mechanism proposed here for maintaining differential rotation in giant planets (and stars) is based on compressional torque instead of vortex stretching torque. Consider a buoyant fluid parcel rising through a density-stratified medium. As it expands it produces a Coriolis torque that causes it to rotate in the opposite direction of the basic rotation of the planet. Note that the Coriolis force due to just the rise of the parcel normal to the rotation axis is balanced by part of the pressure gradient force and so does not generate vorticity; it is the Coriolis torque due to the expansion of the parcel as it rises (i.e., the divergence of the velocity parallel to the equatorial plane) that generates negative vorticity (i.e., an anticyclone) relative to the rotating frame of reference (see equation A4). Likewise, the contraction of a sinking fluid parcel generates positive vorticity (i.e., a cyclone).

One can also describe this process by defining the potential vorticity of the fluid parcel as the total vorticity (twice the planet's rotation rate plus its local vorticity within the rotating frame) divided by its density and can show that this quantity is approximately conserved as the parcel moves (Ertel 1972, Glatzmaier and Gilman 1981). That is, as the density of a rising fluid parcel decreases, its local vorticity also decreases, and vice versa. The derivation of this theorem (see Appendix B) includes the nonlinear inertial term in addition to the pressure gradient and Coriolis terms in the momentum equation and therefore is more appropriate for describing rotating turbulent flows than the linear steady-state Proudman-Taylor theorem.

Turbulent convection clearly does not have the traditional large-scale cellular structure seen in laminar convection. Instead, one needs to consider the motion and deformation of small isolated plumes that gain and lose vorticity as they sink and rise, respectively. The density-stratification mechanism for maintaining differential rotation is based on the resulting tilted flow trajectories which transport angular momentum from one region to another.

#### 3.1 Two models with different radial profiles of density

As a simple demonstration, we present two numerical simulations of strongly turbulent thermal convection in the equatorial plane of a rotating density-stratified planet. The model is two-dimensional (2D), i.e., there are no flows or gradients perpendicular to the plane of the rotating disk. It allows convection down to a solid core at 20% of the outer boundary. To keep this model simple, the outer boundary is set at the radius where the density is just seven times smaller than that at the inner boundary. The anelastic equations of motion are solved using a spectral semi-implicit method (see Appendix A). The spatial resolution is 4096 Fourier grid points in longitude by 1537 Chebyshev grid levels in radius. Each case was run for more than 2,000,000 numerical time steps, representing more than 1000 rotation periods.

Several traditional nondimensional parameters characterize these simulations:

$$\text{Ra} = \frac{g|\partial\rho/\partial S|\Delta S D^3}{\rho\nu\kappa} \quad , \quad \text{Ek} = \frac{\nu}{2\Omega D^2} \quad , \quad \text{Pr} = \frac{\nu}{\kappa} \quad .$$

Here,  $g$  is gravitational acceleration,  $\rho$  is density,  $S$  is specific entropy,  $\Delta S$  is the drop in  $S$  across the depth  $D$  of the convection zone,  $\nu$  is viscous diffusivity,  $\kappa$  is thermal diffusivity and  $\Omega$  is the planetary rotation rate. Values of these variables at mid-depth are used in the nondimensional numbers. The Rayleigh number (Ra), a measure of convective driving relative to viscous and thermal diffusion, is  $3 \times 10^{11}$  and the Ekman

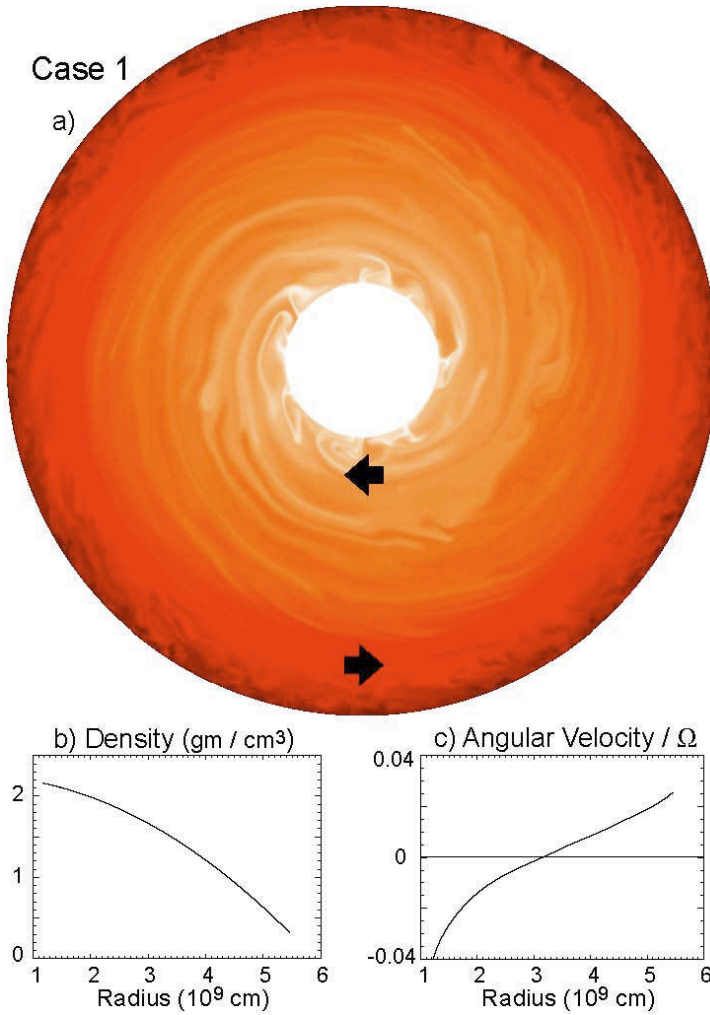


Figure 1. 2D convection and differential rotation, case 1. a. A snapshot of the thermal (entropy) perturbations in a 2D model of the equatorial plane of a giant planet. This is viewed in the rotating frame, down from the northern hemisphere; the planetary rotation is counter-clockwise. The arrows indicate the direction of the zonal flow relative to the rotating frame; the clockwise-directed arrow represents negative (retrograde) angular velocity. Light colors represent hot, buoyant fluid; dark colors represent cold, heavy fluid. b. The prescribed reference state density profile. c. The time averaged angular velocity relative to the rotating frame and scaled by the planetary rotation rate.

number ( $Ek$ ), a measure of viscous to Coriolis effects, is  $10^{-8}$ . The Prandtl number ( $Pr$ ), viscous relative to thermal diffusion, is 0.2. A convenient combination of these numbers, the convective Rossby number ( $Rc$ ), estimates buoyancy to Coriolis effects without considering diffusive effects:

$$Rc = \left( \frac{Ra}{Pr} \right)^{1/2} Ek \quad .$$

In these simulations  $Rc$  is about  $10^{-2}$ ; i.e., Coriolis forces are typically a hundred times greater than buoyancy forces.

The resulting zonal wind amplitude,  $V$ , relative to the rotating frame of reference is a few hundred thousand times greater than the viscous diffusion velocity (i.e., the Reynolds number ( $Re$ ) is roughly  $10^5$ ) and is a hundred times smaller than the velocity of the rotating frame (i.e., the Rossby number ( $Ro$ ) is  $10^{-2}$ ), where

$$Re = \frac{VD}{\nu} \quad , \quad Ro = \frac{V}{2\Omega D} \quad .$$

Convective velocities are typically two orders of magnitude smaller than the surface zonal winds they

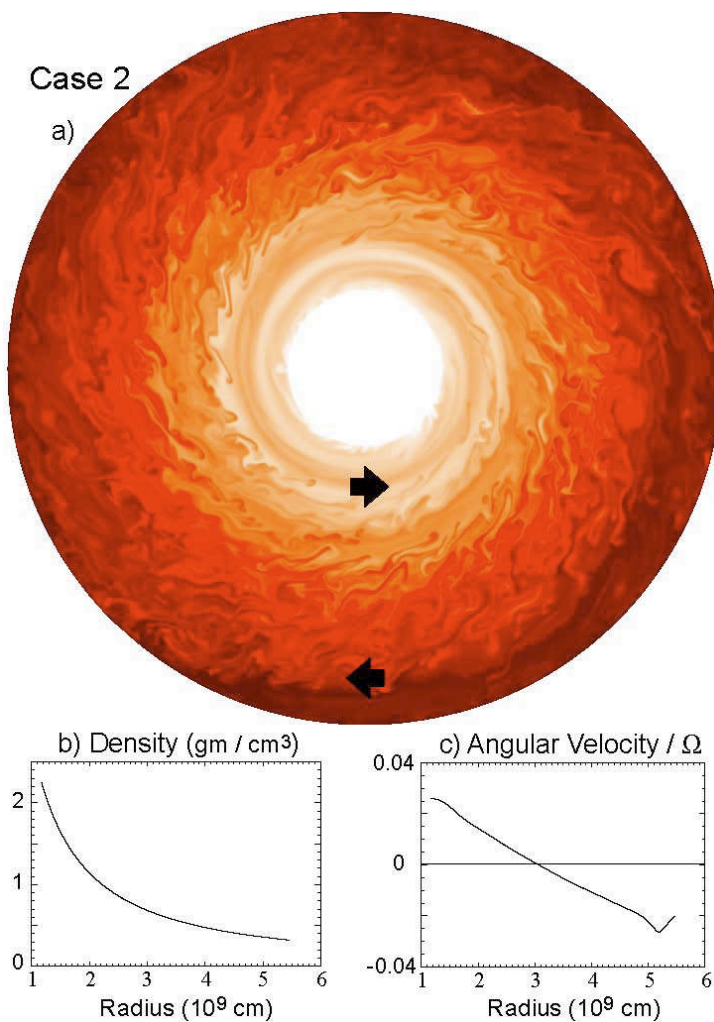


Figure 2. 2D convection and differential rotation, case 2. As in figure 1.

maintain.

These test cases are ideal because if there were no density stratification in this 2D configuration the Coriolis forces would be completely balanced by part of the pressure gradient (see equation A4) and would therefore generate no vorticity and no differential rotation. Also, since there is no flow perpendicular to the 2D plane the longitudinally averaged radial flow vanishes and so there is no thermal wind effect. Therefore, the differential rotation maintained in these simulations is driven entirely by the density-stratification mechanism. The two cases are given the same control parameters and the same total density drop (a factor of seven) across the convection zone but different radial profiles of density. The relative change in density with radius is greatest in Case 1 (figure 1b) near the outer boundary; whereas in Case 2 (figure 2b) it is greatest near the inner boundary.

The density-stratification mechanism for maintaining differential rotation involves a radially-dependent phase propagation in longitude of the vorticity pattern, which tilts the plume trajectories in longitude and thus redistributes angular momentum in radius. To understand how this happens think of the series of upflows and downflows at the onset of convection as convection cells. Positive vorticity peaks in the centers of counter-clockwise circulating cells (cyclones) and negative vorticity peaks in the centers of clockwise circulating cells (anticyclones), when viewed in the rotating frame from the north. However, the rate that vorticity is being generated peaks in the upflows and downflows between the cell centers, i.e.,  $90^\circ$  out of phase relative to the existing pattern of vorticity.

Since rising fluid generates anticyclonic vorticity on the prograde side of anticyclones and on the retrograde side of cyclones, the phase of this circulation pattern propagates in the prograde direction (Glatzmaier and Gilman 1981). This Rossby-like vorticity wave occurs because density decreases with radius.

Consider Case 1. Since the relative decrease in density with radius *increases* with radius in this case, the pattern of circulation propagates eastward faster at greater radii. This causes rising fluid to tilt eastward (i.e., prograde) and sinking fluid to tilt westward (i.e., retrograde). That is, prograde angular momentum is transported toward the outer boundary and retrograde angular momentum is transported away from the outer boundary. The opposite occurs at the inner boundary. This convergence of Reynolds stress maintains prograde zonal flow in the outer part of the convection zone and retrograde flow in the inner part (figure 1c). Once the differential rotation is established it provides positive nonlinear feedback. That is, rising and sinking plumes are sheared by the differential rotation, which increases the tilt and tightens the spiral flow structure. For Case 2, the relative decrease in density with radius *decreases* with radius; therefore the eastward phase propagation is faster at greater depth, which establishes the opposite spiral tilt and differential rotation (figure 2).

Notice that the flow in Case 1 (figure 1a) appears much less turbulent than that in Case 2 (figure 2a). This is likely related to the *Rayleigh Stability Criterion* for a differentially-rotating inviscid fluid disk. For centrifugal force not to exceed gravitational and pressure gradient forces when a fluid parcel is displaced outward, the radial gradient of specific angular momentum in the disk,  $r^2\Omega(r)$ , needs to be positive. Here,  $\Omega(r)$  is the total angular velocity of the fluid disk in the inertial frame. Although this stability criterion is satisfied everywhere for both cases, the positive gradient of  $\Omega(r)$  for Case 1 (figure 1c) makes it more stable than Case 2 (figure 2c); that is, Case 1 provides greater restoring forces against radial displacements.

The evolution of turbulent buoyant parcels detaching from the boundary layers, being differentially torqued by Coriolis forces due to their expansion or contraction, and ultimately establishing a strong differential rotation is clearly seen in computer graphical movies of the two cases presented here (<http://es.ucsc.edu/~glatz/diskmovies>). The structure of this highly-turbulent rotationally-dominated flow is a superposition of small-amplitude non-axisymmetric radial motions (figures 1a and 2a) and the large-amplitude axisymmetric differential rotation (figures 1c and 2c); the result is a series of wave-like flows in longitude. When viewed in the rotating frame of reference, defined as the one with zero total angular momentum, the differential rotation continually winds the thermal spiral patterns. On average, the inner and outer regions make one revolution in opposite directions about every fifty planetary rotation periods. This rate likely depends on the convective Rossby number,  $Rc$ .

The robust feature of the density-stratification mechanism presented here is that it acts locally. It generates vorticity and maintains differential rotation even in a strongly turbulent and magnetic environment without requiring vortex columns spanning the entire interior.

Unlike Jupiter and Saturn, the ice giants, Uranus and Neptune, have westward (retrograde) equatorial zonal winds at their cloud tops, which may be maintained by shallow atmospheric flows (e.g. Williams 1978, Cho and Polvani 1996). Alternatively, a density profile with a steep gradient well below the surface at the liquid-gas transition, as predicted in models of Uranus and Neptune (Hubbard *et al.* 1991), might maintain the westward equatorial zonal wind at the surface as in figure 2 if the density scale height at the transition were smaller than that near the surface.

### 3.2 A fully convective model with no solid core

One-dimensional evolutionary models of Jupiter cannot definitely say that this planet has a rocky core (Hubbard *et al.* 1999, Guillot 1999). It is also likely that some extra-solar giant planets, at least during parts of their lifetimes, are fully convective with no solid core (Bodenheimer *et al.* 2003, Guillot 2005). Therefore it is interesting to compare the flow structures predicted for fully convective giant planets to those with rocky cores.

Numerical simulations using a 2D anelastic finite-volume model of the equatorial plane of a giant planet with no solid core also demonstrate that differential rotation in radius is maintained by the density-stratification mechanism (Evonuk and Glatzmaier 2006, 2007). These studies illustrate how the structure of the convection and zonal flow are significantly influenced by the presence or absence of a solid core when the effects of planetary rotation are small (i.e., for large convective Rossby number,  $Rc$ ). In particular, a dominant dipolar flow is preferred; that is, a flow straight through the center since this is the most efficient way of removing heat from the central region. However, when Coriolis forces are relatively significant (small



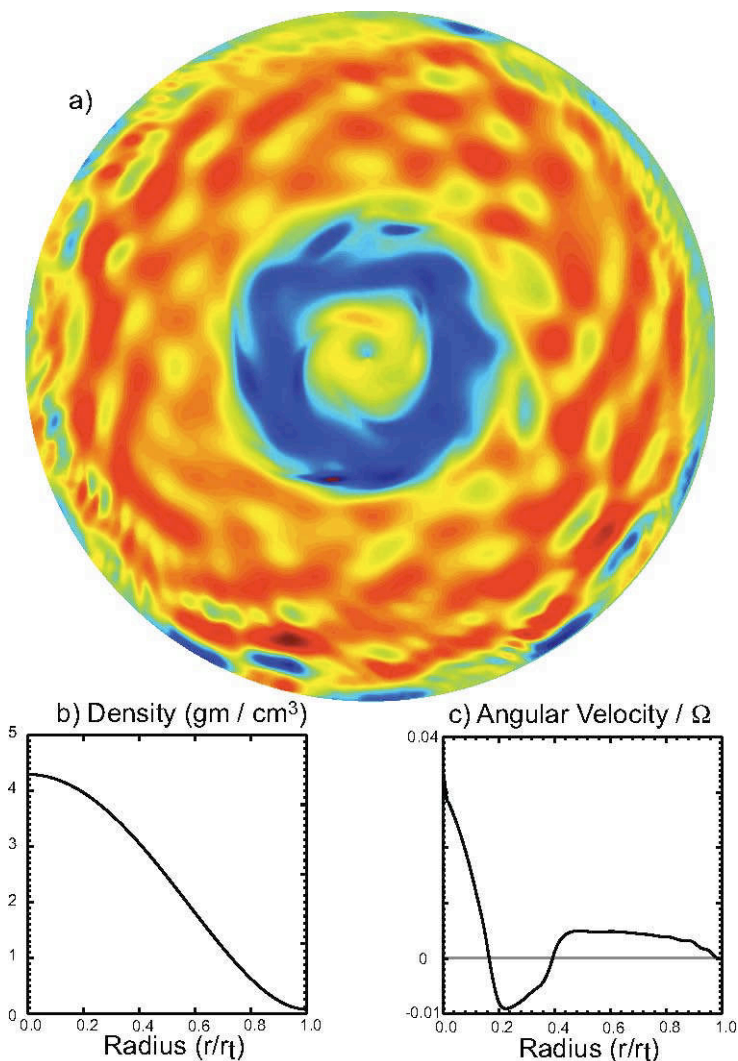


Figure 3. 2D convection and differential rotation without an inner core. a. A snapshot of the angular velocity in a 2D model of the equatorial plane of a giant planet, viewed in the rotating frame with planetary rotation counter-clockwise. Red and yellow indicate prograde angular velocity; blue is retrograde. This case shows three alternating bands of zonal flow. b. The prescribed reference state density profile. Radius is indicated as a fraction of the outer boundary radius. Density at the center is 54.6 times greater than that at the outer boundary. c. The time averaged angular velocity relative to the rotating frame and scaled by the planetary rotation rate.

$Rc$ ) the flow is dominated by the zonal flow.

Simulations with this model (Evonuk 2008) have also shown that the number of alternating bands (in radius) of angular velocity (relative to the mean rotation rate) increases as the  $Rc$  decreases. Figure 3 illustrates a case with three alternating bands in radius. The parameters for this case (with  $D$  being the full radius) are  $Ra = 10^{12}$ ,  $Ek = 10^{-7}$ ,  $Pr = 1$  and therefore  $Rc = 0.1$ . The reference state density at the center is 54.6 times greater than that at the outer boundary (figure 3b); its radial derivative vanishes at both the center and at the outer boundary. The density scale height is minimum in the outer part of the convection zone, which maintains prograde zonal flow there and retrograde flow below (figures 3a,c). The central region has significant prograde angular velocity because the advection of vorticity through this region is by the dipolar flow (i.e., longitudinal wavenumber one). This brings in prograde vorticity (since sinking fluid generates positive vorticity) and removes retrograde vorticity (since rising fluid generates negative vorticity). Similar simulations but with slightly larger  $Rc$  produce only two alternating bands; simulations with much larger  $Rc$  produce a dipolar flow structure.

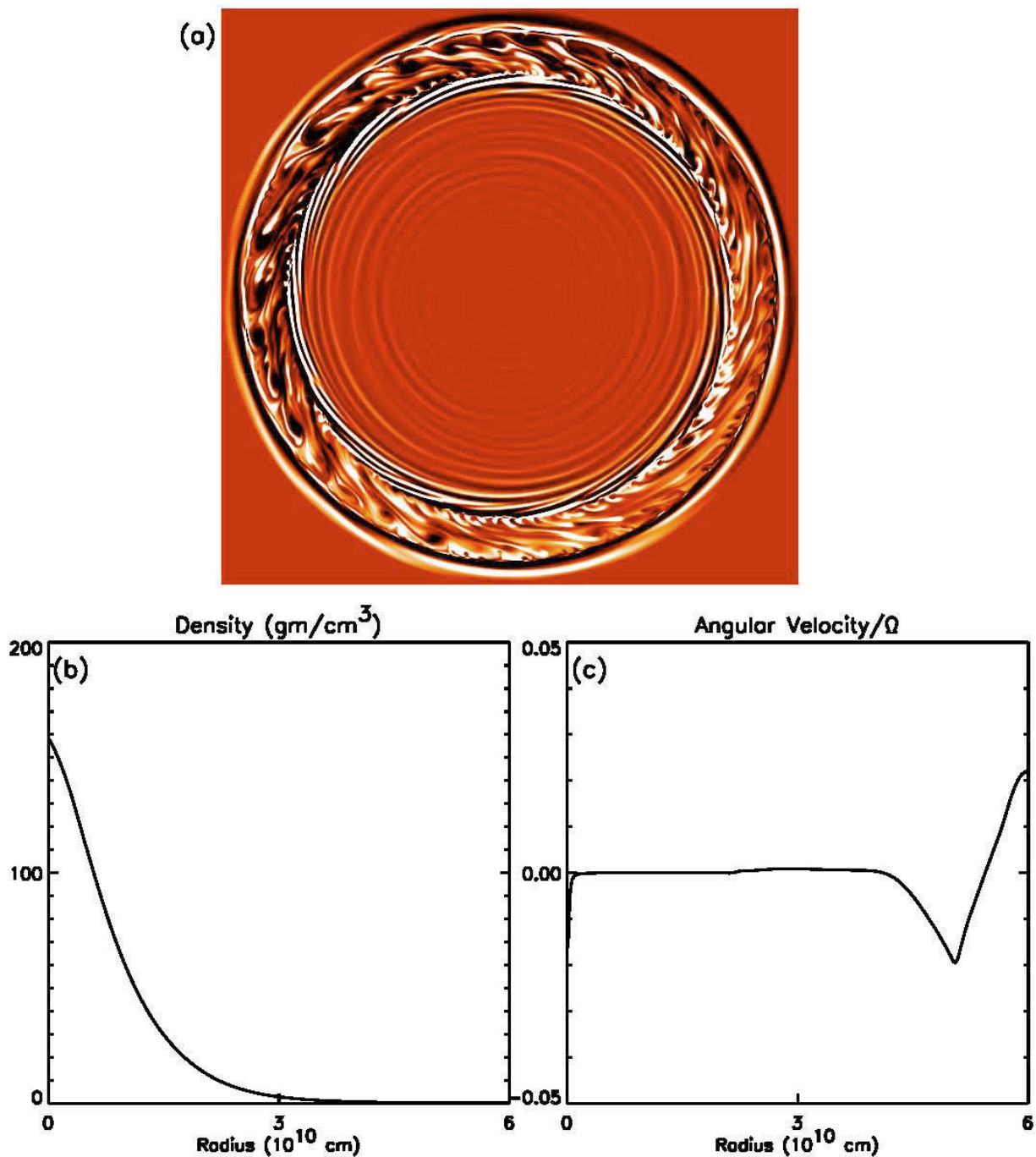


Figure 4. a. A snapshot of the temperature perturbations (relative to the radially-dependent reference state temperature) in a 2D model of rotating convection in the equatorial plane. As in the other figures, rotation is counter-clockwise. Convection exists in the outer unstable (superadiabatic) region and gravity waves in the inner stable (subadiabatic) region. Light colors represent hot, buoyant fluid; dark colors represent cold, heavy fluid. b. The prescribed reference state density profile; density varies by a factor of 20 within the convection zone. c. The time averaged angular velocity relative to the rotating frame and scaled by the planetary rotation rate.

### 3.3 A model with a stable interior below a convection zone

It is likely that some extra-solar giant planets have a convectively stable interior below an unstable convection zone, as does the sun. To study such a scenario, we use another 2D anelastic model within the equatorial plane (Rogers *et al.* 2006). This model employs a spectral method in longitude and a finite-difference method in radius. Only the outer 20% in radius is convectively unstable; a very stable (subadi-

abatic) radiative region is prescribed below the convection zone. A shallow stable layer is also prescribed above the unstable convection zone. The reference state density, pressure and temperature are fitted to a one-dimensional solar evolutionary model. The radii of the model's inner boundary, its stable-unstable interface and its outer boundary are  $0.05R_{sun}$ ,  $0.71R_{sun}$  and  $0.85R_{sun}$ , respectively, where  $R_{sun}$  is the radius of the solar photosphere. The corresponding densities at these radii are 153, 0.20 and  $0.01 \text{ gm cm}^{-3}$ . The Ra, Ek and Pr depend on radius; within the lower part of the convection zone these are  $10^8$ ,  $10^{-6}$  and  $10^{-2}$ , respectively.

A snapshot of the temperature perturbation in the equatorial plane from one of these simulations is illustrated in figure 4, showing tilted plumes in the convection zone and gravity waves in radiative interior. As in the previous cases, differential rotation in the convection zone is maintained by the density-stratification mechanism. Since the density scale height is smallest near the surface in this model as it is in the sun, eastward (prograde) zonal flow is maintained near the surface and westward (retrograde) flow near the base of the convection zone.

Kinetic energy and angular momentum are transferred from downwelling plumes in the convection zone to gravity waves in the stable interior. The dissipation of these waves contributes to the maintenance of a zonal flow in the upper part of the stable interior (figure 4c). This transfer of energy and momentum to the interior reduces the amplitude of the zonal flow in lower part of the convection zone compared to what would be maintained by a stress-free impermeable boundary at the base of the convection zone (Rogers and Glatzmaier 2005).

#### 4 Discussion

It is interesting to compare and contrast the classic vortex-stretching mechanism (Busse 1983, 2002) with the density-stratification mechanism described here. Vorticity is generated in both by Coriolis torques that occur as fluid diverges in planes parallel to the equatorial plane. This occurs for the vortex-stretching scenario because of conservation of fluid volume; that is, fluid in geostrophic convective columns (spanning from the impermeable outer boundary in the northern hemisphere to that in the southern hemisphere) is forced to spread out as it circulates away from the axis of rotation due to sloping ends of the columns determined by the curvature of the spherical boundary. For the density-stratification mechanism, on the other hand, a compressible fluid parcel expands as it rises because of the decrease in the local pressure.

In addition, both mechanisms require the flow trajectories to be tilted in longitude to achieve a convergence of prograde angular momentum in one region and a convergence of retrograde angular momentum in another. For the vortex-stretching mechanism, prograde zonal flow is maintained where the natural logarithm of *column length* decreases most rapidly with *cylindrical* radius. For a spherical outer boundary (outside the tangent cylinder to the inner core) this occurs in the outer part of a convective column, which causes upflow to tilt in the prograde direction and downflow to tilt in the retrograde direction. In particular, this mechanism always produces a prograde zonal flow near the spherical surface in the equatorial region. Note that a retrograde equatorial surface flow could be maintained in a rotating *cylinder* filled with a constant density fluid if the ends have a *concave* shape because eastward-propagating vorticity waves would travel faster near the inner boundary, causing convective columns to be tilted in the opposite direction (Busse 2002). For the density-stratification mechanism, prograde flow is maintained within a convecting region where the natural logarithm of *density* decreases most rapidly with *spherical* radius, which is typically in the outer part of a stratified convecting region for a gas giant. Note, however, that the retrograde tilted upflow and retrograde equatorial zonal flow of our Case 2 (figure 2), which we produce with a “concave-shaped” density profile, is similar in principle to Busse’s (2002) example of “concave-shaped” cylinder boundaries. Therefore, one of the differences between the two mechanisms is that the resulting differential rotation depends on the geometry of the inner and outer impermeable boundaries for the vortex-stretching mechanism; whereas, for the density-stratification mechanism the resulting differential rotation depends on the internal density structure of the planet.

This difference between the two mechanisms is particularly critical for strongly turbulent convection, like that in a giant planet. The vortex-stretching mechanism assumes nonlinear Reynolds stresses are too small to produce instabilities and therefore assumes straight convective columns with sloping (convex) ends

in contact with the impermeable outer boundaries. However, in a strongly turbulent environment these long thin columns would likely not remain straight and intact if they ever do develop. Instead many short disconnected vortices or vortex sheets would likely exist, most not in contact with the outer boundary. Without the organized vortex stretching of the classic mechanism, a stable differential rotation profile may be difficult to maintain in a turbulent constant-density fluid. However, short isolated vortices in a turbulent density-stratified environment can easily maintain a stable differential rotation profile because this mechanism acts locally.

The degradation of differential rotation as convection, in a fluid with a constant background density, becomes increasingly turbulent has been seen in laboratory experiments (e.g. Hart *et al.* 1986, Aubert *et al.* 2001) and in 3D numerical simulations (e.g. Christensen 2002). As the convective Rossby number,  $R_c$ , increases convection becomes more turbulent and the fluid velocities that compose the Reynolds stress become less correlated, reducing the kinetic energy of the differential rotation relative to that of the convection. Christensen (2002) finds that a fairly stable differential rotation profile can however be maintained even when the convective columns and the resulting Reynolds stresses are intermittent in space and time, if there is a robust time-averaged vortex-stretching mechanism. The de-correlation in the velocities seen in these Boussinesq simulations occurs less near the surface where vortices still “feel” the sloping impermeable boundary. As mentioned, vortices in a turbulent density-stratified environment do not need to be deformed by the boundary to maintain a differential rotation.

Several differences between Boussinesq and density-stratified convection also exist in the details of the flow structures. It is easy to see that the global circulation of fluid parcels that expand by several orders of magnitude while rising would have a significantly different pattern than the circulation of constant density fluid. For example, consider the difference between the cylindrical geometry of the vortex-stretching mechanism and the spherical geometry of the density-stratification mechanism. A secondary flow toward the equatorial plane forced by a constant-density convecting column between sloping boundaries causes the fluid to spread out and therefore produces negative vorticity. However, a similar flow trajectory in a density-stratified environment causes a fluid parcel to contract (because spherical radius decreases) and therefore produces positive vorticity. In the polar regions vorticity generation due to a secondary flow toward the equatorial plane is vanishingly small for the Boussinesq vortex-stretching scenario. However, for the density-stratified scenario fluid rising and sinking parallel to the axis of rotation in the polar region expands and contracts as much as it does when flowing within the equatorial plane (over the same spherical radii) and therefore produces considerable vorticity. These differences in flow patterns are particularly important at shallow depths below the surface of a giant gas planet where the volume of a fluid parcel changes significantly as the parcel flows through many density scale heights.

Some high-resolution 3D Boussinesq simulations of convection and differential rotation in giant gas planets (e.g. Heimpel *et al.* 2005) produce surface zonal winds that appear amazingly realistic. However, because of their neglect of density stratification, the structure of convection and zonal winds below their model’s surface may not be as realistic. A convenient test (Glatzmaier 2008) would be to specify Jupiter’s radius and basic rotation period as length and time scales and produce surface zonal winds with roughly the same amplitude and pattern observed on Jupiter. Then, using a realistic depth-dependent electrical conductivity for this semi-conducting region (Liu *et al.* 2008) and the model’s subsurface fluid flow generate a magnetic field similar in amplitude and structure (above the surface) to Jupiter’s observed field. A necessary condition for the subsurface flow to be realistic is to be able accomplish this without generating more Ohmic heating than Jupiter’s observed luminosity.

## 5 Conclusions

We have argued that the extremely thin convective columns required to span from the northern to southern boundaries in the classical vortex-stretching mechanism would likely not develop in the turbulent interiors of giant planets. As an alternative, we have investigated the maintenance of differential rotation due to the effects of rising fluid expanding and sinking fluid contracting within a density-stratified equatorial plane of a giant planet. Our simple 2D computer simulations illustrate how this density-stratification mechanism can maintain differential rotation by compressional torques acting locally on small convective plumes. We

have discussed differences in the flow structures produced with constant-density (Boussinesq) models and those produced by density-stratified (anelastic) models, which are most significant in the outer region of a giant planet where the density scale heights are smallest.

The opposite differential rotation profiles illustrated in figures 1 and 2 suggest that the oppositely directed equatorial winds observed on our ice giants compared to those on our gas giants might be due to their different radial profiles of density (Hubbard *et al.* 1991, Guillot 2005). Our models also demonstrate how this mechanism can maintain differential rotation in radius when the interior is fully convective (i.e., no solid core) and within a convection zone above a convectively stable interior.

The 2D models we have presented here, however, are meant to simply demonstrate this fundamental mechanism, which has been neglected in most previous models of giant planets; they are not meant to predict the pattern or extent of differential rotation below the surface of a giant planet. Our Cases 1 and 2 span only two density scale heights, not the much larger number which exist within a giant planet, most of which occur in the shallow layers where the density-stratification mechanism is most effective. We have also neglected the hydrogen phase transition, which is predicted to exist at roughly 90% of Jupiter's radius and 50% of Saturn's radius (Nellis 2000), and the magnetic field that is generated in the outer semi-conducting region where the electrical conductivity rapidly increases with depth. In addition, we have not addressed the maintenance of differential rotation in latitude, which would require a 3D global simulation with a density stratification in spherical radius.

## Acknowledgments

We thank F. Busse, U. Christensen, C. Jones, P. Olson, P. Roberts and D. Stevenson for discussions. T.R. is supported by an NSF Astronomy and Astrophysics Postdoctoral Fellowship under award 0602023. Support for this research was provided by grants from the NASA *Planetary Atmospheres Program* (NAG5-11220), the NASA *Outer Planets Research Program* (NNG05GG69G), the NASA *Solar and Heliospheric Physics Program* (NNG06GD44G) and from the *Institute of Geophysics and Planetary Physics* at Los Alamos National Laboratory and the University of California Santa Cruz. Computing resources were provided by NSF at the *Pittsburgh Supercomputing Center* and by an MRI funded Beowulf cluster at UCSC (AST-0521566), by the NASA *Advanced Supercomputing Division* and by DOE at the *National Energy Research Scientific Computing Center*.

## References

- Allison, M., A similarity model for the windy jovian thermocline. *Planet. Space Sci.*, 2000, **48**, 753-774.
- Atkinson, D.H., Pollack, J.B. and Seiff, A., The Galileo probe doppler wind experiment: Measurement of the deep zonal winds on Jupiter. *J. Geophys. Res.*, 1998, **103**, 22911-22928.
- Aubert, J., Brito, D., Nataf, H.-C., Cardin, P. and Masson, J.-P., A systematic experimental study of rapidly rotating spherical convection in water and liquid gallium. *Phys. Earth Planet. Inter.*, 2001, **128**, 51-74.
- Bodenheimer, P., Laughlin, G. and Lin, D.N.C., On the radii of extrasolar giant planets. *Astrophys. J.*, 2003, **592**, 555-563.
- Braginsky, S.I. and Roberts, P.H., Equations governing core convection and the geodynamo. *Geophys. Astrophys. Fluid Dyn.*, 1995, **79**, 1-97.
- Busse, F.H., Thermal instabilities in rapidly rotating systems. *J. Fluid Mech.*, 1970, **44**, 441-460.
- Busse, F.H., A model of mean zonal flows in the major planets. *Geophys. Astrophys. Fluid Dyn.*, 1983, **23**, 153-174.
- Busse, F.H., Asymptotic theory of convection in a rotating, cylindrical annulus. *J. Fluid Mech.*, 1986, **173**, 545-556.
- Busse, F.H., Convective flows in rapidly rotating spheres and their dynamo action. *Phys. Fluids*, 2002, **14**, 1301-1314.
- Cho, J.Y.-K. and Polvani, L.M., The morphogenesis of bands and zonal winds in the atmospheres on the giant outer planets. *Science*, 1996, **273**, 335-337.
- Christensen, U.R., Zonal flow driven by strongly supercritical convection in rotating spherical shells. *J. Fluid Mech.*, 2002, **470**, 115-133.

- Dormy, E., Jault, D. and Soward, A.M., A super-rotating shear layer in magnetohydrodynamic spherical Couette flow. *J. Fluid Mech.*, 2002, **452**, 263-291.
- Dowling, T.E., Dynamics of jovian atmospheres. *Ann. Rev. Fluid Mech.*, 1995, **27**, 293-334.
- Ertel, H., Ein neuer hydrodynamischer Wirbelsatz. *Meteorolol. Z.*, 1972, **59**, 277-281.
- Evonuk, M., The role of density stratification in generating zonal flow structures in a rotating fluid. *Astrophys. J.*, 2008, **673**, 1154-1159.
- Evonuk, M. and Glatzmaier, G.A., A 2D study of the effects of the size of a solid core on the equatorial flow in giant planets. *Icarus*, 2006, **181**, 458-464.
- Evonuk, M. and Glatzmaier, G.A., The effects of small solid cores on deep convection in giant planets. *Planet. Space Sci.*, 2007, **55**, 407-412.
- Gilman, P.A. and Glatzmaier, G.A., Compressible convection in a rotating spherical shell I. Anelastic equations. *Astrophys. J. Suppl.*, 1981, **45**, 335-349.
- Glatzmaier, G.A., Numerical simulations of stellar convective dynamos. I. The model and method. *J. Comp. Phys.*, 1984, **55**, 461-484.
- Glatzmaier, G.A., Planetary and stellar dynamos: challenges for next generation models. In *Fluid Dynamics and Dynamos in Astrophysics and Geophysics*, edited by A.M. Soward, C.A. Jones, D.W. Hughes and N.O. Weiss, Chp. 11, pp. 331-357, 2005 (CRC Press: London).
- Glatzmaier, G.A., A note on "Constraints on deep-seated zonal winds inside Jupiter and Saturn". *Icarus*, 2008, in press.
- Glatzmaier, G.A. and Gilman, P.A., Compressible convection in a rotating spherical shell. III. Analytic model for compressible vorticity waves. *Astrophys. J. Suppl.*, 1981, **45**, 381-388.
- Glatzmaier, G.A. and Gilman, P.A., Compressible convection in a rotating spherical shell. V. Induced differential rotation and meridional circulation. *Astrophys. J.*, 1982, **256**, 316-330.
- Guillot, T., A comparison of the interiors of Jupiter and Saturn. *Planet. Space Sci.*, 1999, **47**, 1183-1200.
- Guillot, T., The interiors of giant planets: Models and outstanding questions. *Ann. Rev. Earth Planet. Sci.*, 2005, **33**, 493-530.
- Hammel, H.B., de Pater, I., Gibbard, S., Lockwood, G.W. and Rages, K., Uranus in 2003: Zonal winds, banded structure, and discrete features. *Icarus*, 2005, **175**, 534-545.
- Hart, J.E., Glatzmaier, G.A. and Toomre, J., Spacelaboratory and numerical simulations of thermal convection in a rotating hemispherical shell with radial gravity. *J. Fluid Mech.*, 1986, **173**, 519-544.
- Heimpel, M., Aurnou, J. and Wicht, J., Simulation of equatorial and high-latitude jets on Jupiter in a deep convection model. *Nature*, 2005, **438**, 193-196.
- Hubbard, W.B., Nellis, W.J., Mitchell, A.C., Holmes, N.C., Limaye, S.S. and McCandless, P.C., Interior structure of Neptune: Comparison with Uranus. *Science*, 1991, **253**, 648-651.
- Hubbard, W.B., Guillot, T., Marley, M.S., Burrows, A., Lunine, J.I., Saumon, D.S., Comparative evolution of Jupiter and Saturn. *Planet. Space Sci.*, 1999, **47**, 1175-1182.
- Ingersoll, A.P. and Pollard, D., Motion in the interiors and atmospheres of Jupiter and Saturn: Scale analysis, anelastic equation, barotropic stability criterion. *Icarus*, 1982, **52**, 62-80.
- Ingersoll, A.P., Gierasch, P.J., Banfield, D., Vasavada, A.R. and the Galileo Imaging Team, Moist convection as an energy source for the large-scale motions in Jupiter's atmosphere. *Science*, 2000, **403**, 630-632.
- Liu, J., Goldreich, P.M. and Stevenson, D.J., Constraints on deep-seated zonal winds inside Jupiter and Saturn. *Icarus*, 2008, in press.
- Nellis, W.J., Metallization of fluid hydrogen at 140 GPa (1.4 Mbar): implications for Jupiter. *Planet. Space Sci.*, 2000, **48**, 671-677.
- Porco, C.C., West, R.A., McEwen, A. et al., Cassini imaging of Jupiter's atmosphere, satellites, and rings. *Science*, 2003, **299**, 1541-1547.
- Proudman, J., On the motion of solids in a liquid possessing vorticity. *Proc. R. Soc. Lond. A*, 1916, **92**, 408-424.
- Rhines, P.B., Waves and turbulence on a beta-plane. *J. Fluid Mech.*, 1975, **69**, 417-443.
- Roberts, P.H., On the thermal instability of a rotating-fluid sphere containing heat sources. *Philos. Trans. R. Soc. London*, 1968, **263**, 93-117.

- Rogers, T.M. and Glatzmaier, G.A., Penetrative convection within the anelastic approximation. *Astrophys. J.*, 2005, **620**, 432-441.
- Rogers, T.M., Glatzmaier, G.A. and Jones, C.A., Numerical simulations of penetration and overshoot in the sun. *Astrophys. J.*, 2006, **653**, 766-773.
- Sanchez-Lavega, A., Rojas, J.F. and Sada, P.V., Saturn's zonal winds at cloud level. *Icarus*, 2000, **147**, 405-420.
- Stanley, S. and Bloxham, J., Convective-region geometry as the cause of Uranus' and Neptune's unusual magnetic fields. *Nature*, 2004, **428**, 151-153.
- Starchenko, S.V. and Jones, C.A., Typical velocities and magnetic field strengths in planetary interiors. *Icarus*, 2002, **157**, 426-435.
- Stevenson, D.J., Interiors of the giant planets. *Ann. Rev. Earth Planet. Sci.*, 1982, **10**, 257-295.
- Sun, Z.-P., Schubert, G. and Glatzmaier, G.A., Banded surface flow maintained by convection in a model of the rapidly rotating giant planets. *Science*, 1993, **260**, 661-664.
- Williams, G.P., Planetary circulations: 1. Barotropic representation of Jovian and terrestrial turbulence. *J. Atmos. Sci.*, 1978, **35**, 1399-1424.
- Williams, G.P., Jovian dynamics. Part III: Multiple, migrating, and equatorial jets. *J. Atmos. Sci.*, 2003, **60**, 1270-1296.

## Appendix A: Numerical method

Our models of rotating thermal convection are based on the anelastic equations of motion (e.g. Gilman and Glatzmaier 1981, Braginsky and Roberts 1995), which describe subsonic flow relative to a frame of reference rotating at angular velocity,  $\mathbf{\Omega}$ , and small thermodynamic perturbations relative to a depth-dependent, hydrostatic, adiabatic reference state (here denoted by an over-bar). The equations governing conservation of mass (A.1) and momentum (A.2) and the equation for heat transfer (A.3) are

$$\nabla \cdot (\bar{\rho}\mathbf{v}) = 0 \quad (\text{A1})$$

$$\frac{\partial \mathbf{v}}{\partial t} = -(\mathbf{v} \cdot \nabla)\mathbf{v} - \nabla\left(\frac{p}{\bar{\rho}} + U\right) + \bar{\mathbf{g}} \left(\frac{\partial \bar{\rho}}{\partial S}\right)_p S + 2\mathbf{v} \times \mathbf{\Omega} + \nu \nabla^2 \mathbf{v} \quad (\text{A2})$$

$$\frac{\partial S}{\partial t} = -(\mathbf{v} \cdot \nabla)S + \frac{\kappa}{\bar{\rho}T} \nabla \cdot (\bar{\rho} \bar{T} \nabla S) \quad (\text{A3})$$

where  $\mathbf{v}$  is fluid velocity,  $\bar{\rho}$  is reference state density and  $S$ ,  $p$  and  $U$  are the perturbations in specific entropy, pressure and gravitational potential, respectively. We are using the co-density formulation, which combines the pressure gradient, the pressure contribution to the density perturbation and the gravitational potential perturbation into the gradient of a reduced-pressure,  $(p/\bar{\rho}) + U$  (Braginsky and Roberts 1995). To keep this model relatively simple, we have prescribed constant viscous,  $\nu$ , and thermal,  $\kappa$ , diffusivities, which represent subgrid-scale turbulent diffusion; this is the reason our diffusive heat flux is proportional to the entropy gradient. No hyperdiffusion is employed; that is, these diffusion coefficients do not depend on length scales or wavenumbers. In addition, to keep this model simple we have neglected the additional viscous terms in equation (A.2) that depend on the radial derivative of the reference state density; and in (A.3) we have neglected viscous heating. This should not noticeably affect the results of these low viscosity simulations.

Our 2D model is written in cylindrical coordinates  $(r, \phi, z)$ . It assumes no flows or gradients in the  $z$  direction, the direction of the rotation rate,  $\mathbf{\Omega} = \Omega \hat{z}$ . The reference state density,  $\bar{\rho}$ , is prescribed as simple functions of  $r$ . For Case 1  $\bar{\rho} = c_1 - c_2 r^2$  and for Case 2  $\bar{\rho} = c_3 r^{-1.25}$ , where  $c_1$ ,  $c_2$  and  $c_3$  are

constants. Consequently, the density scale height,  $L_{compress} = -(d \ln(\bar{\rho})/dr)^{-1}$ , decreases with radius for Case 1 and increases with radius for Case 2. Integrating density in radius provides the radially-dependent reference state gravitational acceleration,  $\bar{\mathbf{g}} = -\bar{g}\hat{r}$  in (A.2). The hydrostatic equilibrium equation can then be integrated to get the reference state pressure. An equation of state provides the reference state temperature,  $\bar{T}$ , and the thermodynamic derivative  $(\partial\bar{\rho}/\partial S)_p$ . Here we assume a perfect gas, which makes this thermodynamic derivative equal to  $-\bar{\rho}/c_p$ , where  $c_p$  is the (constant) specific heat capacity at constant pressure.

Since this is a 2D problem, we choose to solve the vorticity equation, i.e., the curl of (A.2). This removes the reduced pressure perturbation term from the calculation. The resulting equation for the z-component of vorticity,  $\omega = (\nabla \times \mathbf{v})_z$ , is

$$\frac{d\omega}{dt} = \frac{\partial\omega}{\partial t} + (\mathbf{v} \cdot \nabla)\omega = \frac{\bar{g}}{r\bar{\rho}} \left( \frac{\partial\bar{\rho}}{\partial S} \right)_p \frac{\partial S}{\partial\phi} - (2\Omega + \omega)\nabla \cdot \mathbf{v} + \nu\nabla^2\omega \quad . \quad (\text{A4})$$

The compressional torque in this equation is, using equation (A.1),

$$-(2\Omega + \omega)\nabla \cdot \mathbf{v} = (2\Omega + \omega)h_\rho v_r \quad ,$$

where  $h_\rho = d \ln(\bar{\rho})/dr$ , the negative of the inverse density scale height,  $L_{compress}$ . The stretching torque,

$$(2\Omega + \omega) \cdot \nabla v_z \quad ,$$

vanishes in this 2D model. We then define a streamfunction,  $\Psi$ , such that

$$\bar{\rho}\mathbf{v} = \nabla \times (\Psi\hat{z}) \quad , \quad (\text{A5})$$

which ensures mass conservation (A.1). Vorticity is therefore

$$\omega = -\frac{1}{\bar{\rho}} \left[ \frac{\partial^2\Psi}{\partial r^2} + \left( \frac{1}{r} - h_\rho \right) \frac{\partial\Psi}{\partial r} + \frac{1}{r^2} \frac{\partial^2\Psi}{\partial\phi^2} \right] \quad . \quad (\text{A6})$$

We make the inner and outer boundaries impermeable and stress-free. The former requires  $v_r$  to vanish and, by (A.5),  $\Psi$  to be constant on these boundaries. We therefore set  $\Psi = 0$  on both boundaries to make the total integrated momentum vanish relative to the rotating frame. The latter boundary condition requires the radial gradient of  $(v_r/r)$  to vanish and therefore

$$\left[ \frac{\partial^2\Psi}{\partial r^2} - \left( \frac{1}{r} + h_\rho \right) \frac{\partial\Psi}{\partial r} \right] = 0$$

on both boundaries. We also constrain entropy to be constant on the boundaries; the drop in entropy between the boundaries,  $\Delta S$ , drives the convection.

We expand  $S$ ,  $\omega$  and  $\Psi$  in Fourier functions of  $\phi$  and Chebyshev polynomials of  $r$ . Equations (A.3), (A.4) and (A.6) are solved simultaneously, one complex Fourier mode at a time, using Chebyshev collocation. The time integration treats all linear terms implicitly (including the Coriolis term). The nonlinear advection terms are treated explicitly with the Adams-Bashforth scheme. A spectral transform method, using fast Fourier transforms in both longitude and radius, is employed to calculate the nonlinear terms at each time step. This method is similar to that described in Glatzmaier (1984).

For these anelastic equations, the numerical time step is limited by the CFL condition based on the fluid velocity and the spatial grid. The Chebyshev grid in radius, being much finer near the boundaries,



provides enhanced resolution of the shallow boundary layers without a severe CFL constraint since the radial velocity vanishes at the boundaries.

The code is parallel. For part of each numerical time step the Fourier modes are distributed over the processors so each of the Chebyshev collocation matrix solutions can be done within one processor. During the other part of the step the radial levels are distributed so each of the spectral transforms in longitude can be done within one processor. This requires global transposes each numerical time step, a price one pays for the enhanced accuracy of spectral methods over local finite difference methods.

## Appendix B: Potential vorticity theorem

This theorem is based on the assumption that buoyancy and viscous terms can be neglected to first order in the vorticity equation (A.4). However, unlike the Proudman-Taylor Theorem, the inertial term,

$$\frac{d\omega}{dt} = \frac{\partial\omega}{\partial t} + (\mathbf{v} \cdot \nabla)\omega \quad ,$$

is retained. Since  $\bar{\rho}$  depends only on  $r$ ,  $h_\rho v_r = d \ln \bar{\rho} / dt$ . Also, since  $\Omega$  is constant in space and time,  $\partial\omega/\partial t = \partial(2\Omega + \omega)/\partial t$ . Substituting these into (A.4) gives

$$\frac{d}{dt} \left( \frac{2\Omega + \omega}{\bar{\rho}} \right) = 0 \quad .$$

That is, the potential vorticity of a fluid parcel,  $(2\Omega + \omega)/\bar{\rho}$ , remains constant as the parcel moves. In 3D one would need to neglect the local vortex stretching term to arrive at this result. This, however, may not be negligible in a turbulent density-stratified environment.